



Benefits of assimilating thin sea-ice thickness from SMOS-Ice into the TOPAZ system

Jiping Xie¹, Francois Counillon¹, Laurent Bertino¹, XiangshanTian-Kunze²,
and Lars Kaleschke²

1. Nansen Environmental and Remote Sensing Center, Bergen, Norway
2. Institute of Oceanography, University of Hamburg, German



1
2
3
4
5
6
7
8
9
10
11
12
13
14
15
16
17
18
19
20
21
22
23
24
25
26
27
28
29
30
31

Abstract

An observation product for thin sea ice thickness (SMOS-Ice) is derived from the brightness temperature data of the European Space Agency's (ESA) Soil Moisture and Ocean Salinity (SMOS) Mission, and available in real-time at daily frequency during the winter season. In this study, we investigate the benefit of assimilating SMOS-Ice into the TOPAZ system. TOPAZ is a coupled ocean-sea ice forecast system that assimilates SST, altimetry data, temperature and salinity profiles, ice concentration, and ice drift with the Ensemble Kalman Filter (EnKF). The conditions for assimilation of sea ice thickness thinner than 0.4m are favorable, as observations are reliable below this threshold and their probability distribution is comparable to that of the model. Two paralleled runs of TOPAZ have been performed respectively in March and November 2014, with assimilation of thin sea ice thickness (thinner than 0.4 m) in addition to the standard ice and ocean observational data sets. It is found that the RMSD of thin sea-ice thickness is reduced by 11% in March and 22% in November suggesting that SMOS-Ice has a larger impact during the beginning of freezing season. There is a slight improvement of the ice concentration and no degradation of the ocean variables. The Degrees of Freedom for Signal (DFS) indicate that the SMOS-Ice contents important information (> 20% of the impact of all observations) for some areas in the Arctic. The areas of largest impact are the Kara Sea, the Canadian archipelago, the Baffin Bay, the Beaufort Sea and the Greenland Sea. This study suggests that SMOS-Ice is a good complementary dataset that can be safely included in the TOPAZ system as it improves the ice thickness and the ice concentration but does not degrade other quantities.

Keywords: SMOS-Ice; EnKF; OSE; thin sea-ice thickness; DFS;



1 1. Introduction

2
3 The Arctic climate system has undergone large changes during the last 20
4 years: increase of temperature (Chapman and Walsh, 1993; Serreze et al.,
5 2000; Karl et al., 2015; Roemmich et al., 2015), decrease of sea ice extent
6 (Chapman and Walsh, 1993; Johannessen et al., 1999; Shimada et al., 2006;),
7 sea ice thinning and loss of sea ice volume (Rothrock et al., 1999; Kwok and
8 Rothrock, 2009; Laxon et al., 2013). The interpretation of such changes is
9 severely hampered by the sparseness and the diversity of observational
10 network. The reanalysis database that combines the sparse observations with
11 dynamically consistent modeling is becoming an important tool.
12 While observations of sea ice concentrations have been available for the
13 past 30 years, observations of sea ice thickness are comparatively sparse. An
14 improved knowledge of the ice thickness would be greatly beneficial both for
15 model developments and for improving the accuracy of operational ocean
16 forecasting system. The initialization of sea-ice thickness is also expected to
17 improve predictability on seasonal time scale (Guemas et al. 2014). Until the
18 last decade, observations of sea-ice thickness were mostly limited to field
19 campaigns or submarine measurements. Major efforts in remote sensing have
20 been proposed to monitor the spatiotemporal evolution of ice thickness, and
21 gradually obtained various products from different satellite retrieval algorithms.
22 Measurements of thick sea ice draft on basin-wide scales have been derived
23 from laser altimeters on board ICESat (e.g., Forsberg and Skourup, 2005;
24 Kurtz et al., 2009; Kwok and Rothrock, 2009) or from radar altimeters on ERS,
25 EnviSAT and CryoSat2 (e.g., Laxon et al., 2003; Giles et al., 2008; Connor et
26 al., 2009). Still large uncertainties remain in the accuracy of the resulting ice
27 thickness estimates (larger than 0.5 m) due to uncertainties in the snow depth
28 and the sea ice density (Zygmuntowska et al., 2014). A new database based
29 on Cryostat-2 has been provided (Laxon 2013; Ricker et al., 2014) and has
30 been made available in near real time (Tilling et al. 2016). Finally, methods for
31 sea ice thickness retrieval based on measurements of the brightness
32 temperature at a low microwave frequency of 1.4 GHz (L-band: wavelength
33 $\lambda_a=21$ cm) have been developed in preparation for the European Space
34 Agency's (ESA) Soil Moisture and Ocean Salinity (SMOS) mission (Heygster et



1 al., 2009; Kaleschke et al., 2010). It has been shown that SMOS can be used
2 to retrieve level ice thickness up to half a meter under cold conditions
3 (Kaleschke et al., 2012; Huntemann et al., 2014).

4 An improved retrieval method based on a radiative transfer model and a
5 thermodynamic sea ice model has been further proposed by considering
6 the variations of ice temperature, salinity and a statistical thickness distribution
7 (Tian-Kunze et al., 2014). The operational daily product derived using this
8 method, henceforth called SMOS-Ice, has been validated during a field
9 campaign in the Barents Sea (Kaleschke et al., 2016; Mecklenburg et al.,
10 2016) and will be used in this study. Aiming at the operational application of
11 the thickness measurements for sea ice, the SMOS-Ice data contain daily
12 products of sea ice thickness since the winter of 2010 (Tian-Kunze et al., 2014).
13 Yang et al. (2015) studied the benefit of SMOS-Ice during the freezing period,
14 with the LSEIK (an assimilation method related to the EnKF) in a nested Arctic
15 configuration of the MITgcm. They found that SMOS-Ice leads to improvement
16 of ice thickness and ice concentration. This study is a follow up and assess: 1)
17 the impact of assimilating SMOS-Ice both during the beginnings of melting and
18 freezing seasons; 2) the relative contribution of SMOS-ice compared to a
19 complete set of observations typically used in a state of the art forecasting
20 system.

21 The TOPAZ system is a coupled ocean-sea ice data assimilation system that
22 focuses on the marine environment in the Arctic region. It is the operational
23 Arctic forecast system in the Copernicus Marine Services
24 (<http://marine.copernicus.eu/>). The system provides 10-days coupled physical-
25 biogeochemical forecast every day and long-term reanalysis (Sakov et al.,
26 2012; Lien et al., 2016; Xie et al., 2016). At present, the TOPAZ system
27 assimilates the Sea Surface Temperature (SST), along-track Sea Level
28 Anomalies (SLA) from satellite altimeters, in situ temperature and salinity
29 profiles, Sea Ice Concentration (ICEC) and sea ice drift data from satellites
30 with the Ensemble Kalman Filter (EnKF). The reanalysis product of the TOPAZ
31 system has been widely used in studies about ocean circulation and sea ice in
32 the northern Atlantic Ocean or in the Arctic region (Melsom et al., 2012;
33 Johannessen et al., 2014; Korosov et al., 2015; Lien et al., 2016). However,
34 TOPAZ does not assimilate sea ice thickness, and does not apply postprocess



1 for this variable. In the Arctic reanalysis, the daily sea ice thickness of TOPAZ
2 for the period 1991-2013 has been validated and compared to the
3 observations from ICESat and IceBridge in Xie et al. (submitted in 2016). While
4 the spatial pattern and regression compare reasonably well, the large biases
5 exist. Inaccuracy in the ice thickness is a drawback of coupled ice-ocean
6 models in the Arctic (Johnson et al., 2012; Smith et al., 2015).

7 This paper is organized as follows: section 2 introduces the main
8 components of TOPAZ system including the model, the assimilation scheme,
9 and the observations assimilated. In section 3, we compare SMOS-ice data to
10 the TOPAZ reanalysis for the period 2010-2013, to investigate potential biases
11 and whether conditions are favorable for data assimilation. In section 4, an
12 Observing System Experiment (OSE) is conducted, consisting of two
13 assimilation runs with and without assimilating the SMOS-Ice data during 2014.
14 In Section 5, we compared the contributions of SMOS-Ice relative to other
15 types of observations.

16

17 **2. Descriptions of TOPAZ data assimilation system**

18

19 **2.1 The coupled ice-ocean model**

20

21 The ocean general circulation model used in the TOPAZ system is the version
22 2.2 of the Hybrid Coordinate Ocean Model (HYCOM) developed at University
23 of Miami (Bleck, 2002; Chassignet et al., 2003). HYCOM uses a hybrid vertical
24 coordinate, which smoothly transits from isopycnal layers in the stratified open
25 ocean to z-level coordinates in the unstratified surface mixed layer. This
26 feature has been demonstrated in a wide range of applications from the deep
27 oceans to the shelf (Winther and Evensen, 2006; Chassignet et al., 2009). The
28 NERSC-HYCOM model is coupled to a sea-ice model for which the ice
29 thermodynamics are described in Drange and Simonsen (1996) and the ice
30 dynamics are based on the elastic-viscous-plastic rheology described in
31 Hunke and Dukowicz (1997) and with a modification from Bouillon et al.
32 (2013). TOPAZ uses conformal mapping (Bentsen et al., 1999) and has a
33 quasi-homogeneous horizontal resolution of 12-16 km in the Arctic as shown
34 in Fig. 1.



1 The temperature and salinity at model lateral boundaries are relaxed to a
2 combined climatology between the World Atlas of 2005 (WOA05, Locarnini et
3 al., 2006) and the version 3.0 of the Polar Science Center Hydrographic
4 Climatology (PHC, Steele et al., 2001). A seasonal inflow from the Pacific
5 Ocean through the Bering Strait is imposed, which amplitude is following the
6 observations from Woodgate et al. (2012).

7

8 **2.2 Implementation of the EnKF in TOPAZ**

9

10 The analysis field of model state at time of t_i , is expressed as follows:

$$11 \quad \mathbf{X}_i^a = \mathbf{X}_i^f + \mathbf{K}_i(\mathbf{y}_i - \mathbf{H}_i\mathbf{X}_i^f) \quad (1).$$

12 Where \mathbf{X}_i is the model state vector, the superscripts “a” and “f” refer to the
13 analysis and the forecast respectively. The ensemble consists of 100
14 dynamical members. \mathbf{H}_i is the observation operator and \mathbf{y}_i is the observation
15 vector, which includes all observations at the assimilation time window. The
16 Kalman gain \mathbf{K}_i in Equation (1) is calculated as:

$$17 \quad \mathbf{K}_i = \mathbf{P}_i^f \mathbf{H}_i^T [\mathbf{H}_i \mathbf{P}_i^f \mathbf{H}_i^T + \mathbf{R}_i]^{-1} \quad (2).$$

18 Where \mathbf{R}_i is the matrix of observation error variance, and \mathbf{P}_i is the matrix of
19 background error covariance. The TOPAZ system uses the deterministic EnKF
20 (DEnKF, Sakov and Oke, 2008; Sakov et al., 2012), which is a square-root
21 filter implementation of the EnKF. The covariance \mathbf{P}^a is equal to

$$22 \quad \mathbf{P}_i^a = (\mathbf{I} - \mathbf{K}_i \mathbf{H}_i) \mathbf{P}_i^f + \frac{1}{4} \mathbf{K}_i \mathbf{H}_i \mathbf{P}_i^f \mathbf{H}_i \mathbf{K}_i^T \quad (3)$$

23 Compared to the traditional estimation of the analyzed error covariance, the
24 extra term is quadratic and positive. It induces an overestimation of the
25 analyzed error covariance, which partially compensates the need for ensemble
26 inflation.

27 An overview of the observations assimilated in the present TOPAZ system is
28 given in Table 1 (see as well Sakov et al, 2012; Xie et al., submit in 2016).
29 Observations are quality controlled and superobed as in Sakov et al (2012).
30 The system assimilates the following data set on a weekly basis: the gridded
31 OSTIA SST (Donlon et al., 2012); OSI-SAF ice concentration available for the
32 analysis day; along-track SLA; delayed-mode profiles of temperature and
33 salinity, and the sea-ice drift during the 2 days prior to the analysis. All



1 measurements are retrieved from <http://marine.copernicus.eu>. SLA data and
2 sea ice drift are assimilated asynchronously as described in Sakov et al. (2010)

3

4 **3. Bias analyses for thin ice thickness in TOPAZ**

5

6 TOPAZ provides a reanalysis at daily frequency of physical variables including
7 sea ice thickness, which was validated by in situ and satellite observations in
8 Xie et al. (2016). An assumption made for data assimilation is that the model
9 and observations have unbiased mean and uncertainties estimates. Therefore,
10 we investigate in this section the biases in the thickness of thin sea ice during
11 four winters from 2010-2014.

12 SMOS-Ice products are available since 2010 in the winter months, from 15th
13 October to 15th April. Figure 2 shows the TOPAZ ice thickness as conditional
14 expectations with respect to SMOS-Ice data organized by bin of 5 cm. The
15 TOPAZ equivalent ice thickness is calculated at observations location and time.
16 The error bars show the observation uncertainty (in red) and the TOPAZ
17 RMSD (in cyan) compared to the observations of the bin. Overall, the sea ice
18 thickness in TOPAZ tends to be overestimated. However, the comparison
19 varies largely from month to month as a function of ice thickness,
20 especially for thick ice. As an example, the model overestimates the high
21 thickness values (>0.4 m) during October. However, during November the
22 model underestimates the high thickness values (>0.4 m), while it largely
23 overestimates them in Feb-Apr. For thicknesses lower than 0.4 m, the match
24 between the observations and the simulations of TOPAZ is closer and more
25 consistent through the winter season and in consecutive bins. There is no clear
26 bias from October–December but an increasing thick bias from January–April.
27 There is a priori no indication whether the bias is a model bias or an
28 observation bias. In order to avoid multivariate transfers of bias, whichever the
29 source, the assimilation of SMOS-Ice is restrained to thickness less than 0.4 m.
30 This is also motivated by physical considerations on the wavelength of L-Band
31 microwaves. The penetration depth into sea ice is about 0.5 m at this
32 microwave frequency (Kaleschke et al., 2010; Huntemann et al., 2014), and
33 the effect of ice melting may lead to a saturation thickness of less than 0.4 m,
34 (see Heygster et al. (2009)).



1 Furthermore, relative to the thickness observations of SMOS-Ice for the thin
2 sea ice no more than 0.4 m, the yearly bias in the period 2010-2014 are shown
3 by the black lines in Fig. 3. After 2011, the thick bias is increased, and reaches
4 about 0.1 m in 2014. The thick bias in March is also found larger than that in
5 November. Also the spatial variability of the bias is shown in the right panel of
6 Fig.3, with the bias being largest in the Beaufort Sea and in the Kara Sea. In
7 2014, there is a thick bias in all regions.

8

9 4. Observing System Experiment of SMOS-Ice

10

11

12

4.1 Design of OSE runs for the SMOS-Ice

13

14

15

16

17

18

19

20

21

22

23

24

25

26

27

28

29

30

31

32

33

The SMOS-Ice ice thickness data (version 2.1) is gridded at a resolution of approximately 12.5 km and available at daily frequency in winter months. Only the observations between 0 and 0.4 m, with a distance of at least 30 km away from the coast, are used (See Section 3). The innovations in Equation (1) are expressed as a sea ice volume, which is an additive variable suited for spatial interpolation:

$$\Delta h_{ice} = y_{smos} - \mathbf{H}_i(\mathbf{h}_{mod} \times \mathbf{f}_{mod}) \quad (4)$$

where \mathbf{H} is the bilinear interpolation, h_{mod} and f_{mod} are the model sea ice thickness and concentration respectively. To highlight the additional impacts of observations, two assimilation runs for Observing System Experiment (OSE) are named as follows:

-Official Run: uses the standard observational network of the TOPAZ system. It assimilates weekly the along-track SLA (TSLA), SST, in situ profiles of temperature and salinity, sea-ice concentrations and sea-ice drift data (listed in **Table 1**).

-Test Run: assimilates SMOS-Ice data (version 2.1) in addition to observations assimilated in the official run. The observation error standard deviation of the sea ice thickness uses the uncertainties recommended by the provider, with an upper limit of 5 m beyond which the observations are assumed to have negligible impacts. The observation error is assumed spatially uncorrelated.



1 We have two parallel assimilation runs focusing on two typical time periods
2 within the beginnings of ice melting and freezing, from 19th February to 31th
3 March and from 22th October to 30th November in 2014. Both runs are driven
4 by the same atmospheric high frequency forcing from ERA-Interim (Simmons
5 et al., 2007; Dee et al., 2011). Finally, the daily averaged outputs in March and
6 November are used for the evaluation.

7

8 **4.2 Error analysis in the OSE runs**

9 The analysis focuses on the following target quantities as listed in Table 1: sea
10 ice thickness (from SMOS-Ice), sea ice concentration, SST and SLA. All
11 quantities are calculated from daily averages, and we calculate the bias and
12 the RMSD:

$$13 \quad \text{Bias} = \frac{1}{N} \sum_{i=1}^N (\mathbf{H}_i \bar{\mathbf{X}}_i^f - y_i) \quad (5)$$

$$14 \quad \text{RMSD} = \sqrt{\frac{1}{N} \sum_{i=1}^N (\mathbf{H}_i \bar{\mathbf{X}}_i^f - y_i)^2}, \quad (6)$$

15 where $\bar{\mathbf{X}}_i^f$ is the daily averaged forecast of the model variables, which is
16 compared to the observation on the same location and time.

17

18 The spatial distribution of selected SMOS-Ice data for thin sea ice is shown in
19 the top panels of Fig. 4 during March and November of 2014. In March, the
20 available observations in the Beaufort Sea are very few, and
21 inhomogeneously distributed - mainly located in the coastal estuary areas.
22 Therefore in the following analysis, we will only present the result in the
23 Beaufort Sea for November. In the middle panels of Fig. 4, the differences of
24 RMSD for sea-ice thickness between the **Official Run** and the **Test Run** are
25 shown (red color indicates an improvement due to assimilation of SMOS-Ice).
26 In March, the improvements are mainly found to the east of Franz Josef Land
27 and to some extent near the ice edge in the Greenland Sea. In November, the
28 reduction of RMSD is larger than 0.2 m in the Beaufort Sea, the Greenland
29 Sea and to the north of Svalbard. Finally, the differences of monthly ice
30 thickness between the **Official Run** and the **Test Run** are shown in the



1 bottom panels of Fig. 4. It suggests that the impact of assimilating SMOS-Ice
2 leads to a reduction of sea-ice thickness both in March and November of 2014.
3 The time series of daily bias and RMSD for thin ice thicknesses in the OSE
4 runs are shown in the top panels of Fig. 5. The bias of thin sea-ice thickness is
5 reduced from 16 cm to 12 cm in March, and from 7 cm to 4 cm in November,
6 when SMOS-Ice data is assimilated. The RMSD of thin sea ice is reduced
7 from 35 cm to 31 cm in March, and from 27 cm to 21 cm in November. This
8 corresponds to a reduction of the bias of 25% in March and 43% in November,
9 and a reduction of the RMSD of about 11% in March and 22% in November. In
10 the other panels of Fig. 5, the bias and RMSD of sea ice concentration, SST
11 and SLA are presented. There is a slight benefit for the bias and RMSD of sea
12 ice concentration, but the statistics for SST and SLA are unchanged.
13 Moreover, the time evolution of the averaged thicknesses of thin sea-ice in the
14 marginal seas - in the Kara Sea, Barents Sea and Beaufort Sea - are
15 highlighted with the marked lines in the panels of Fig. 6. The corresponding
16 daily RMSDs of ice thickness relative to thin SMOS-Ice data are added with
17 shading. In each month, there are four assimilations marked with the vertical
18 lines.
19 In the Kara Sea, the thickness observed in March is very stable with a slight
20 gradual increase. There is a relatively uniform reduction of RMSD by about
21 21%, which is mainly the result from a correction of the large (too thick) bias in
22 the model. In November, the bias is much smaller and the resulting
23 improvement is smaller (8%) but the performances are improving slightly
24 through the month for RMSD.
25 In the Barents Sea, in March, the observations show an increasing trend. The
26 official run shows initially a large (thick) bias that is reduced as the thickness
27 increase in the observation. Assimilation of SMOS-Ice data reduces well the
28 initial bias, but the bias converges with the official run at the end of the month
29 and so is the RMSD. On average, the RMSD of ice thickness is decreased
30 about 27% from the **Test Run**. In November, the observations show large
31 variability that is well captured in the **Official Run** but the ice is initially too
32 thick. The RMSD reduction is about 19% from the **Test Run** compared to from
33 the **Official Run** and both the bias and the variability seem to be reduced.



1 In the Beaufort Sea, there are too few observations to provide a representative
2 estimate of the system performance in March (top panels of Fig. 4) and the
3 statistic are not presented. In November, the observations shows an increasing
4 trend and the official run shows once more a relatively large thick bias initially.
5 The RMSD in the **Test Run** is reduced by about 51%, which is mainly caused
6 by a reduction of the bias. The increasing trend in the **Test Run** is in relatively
7 well agreement with the observations.

8

9 **5. Relative impact of SMOS-ice to the existing observation** 10 **network**

11 In this Section, the additional benefit of assimilating SMOS-Ice into the TOPAZ
12 system is quantitatively compared to the standard observation network used.
13 To do so, we evaluate a metric calculated during the analysis, the Degree of
14 Freedom for Signal (DFS), which is now widely used for such purpose
15 (Rodgers, 2000; Cardinali et al., 2004). During the assimilation, one can
16 calculate the DFS as following:

$$17 \quad DFS = tr \left(\frac{\partial \hat{y}}{\partial y} \right) = tr \left\{ \frac{\partial [H(X^a)]}{\partial y} \right\} = tr(KH) \quad (7)$$

18 DFS quantifies the reduction of mode that can be attributed to each
19 observation type. A value of DFS close to 0 means that the observation had no
20 update, while a value of m means that the assimilation has reduced the
21 number of degree of freedom of the ensemble by m . Note that the reduction
22 cannot exceed the ensemble size; i.e. 100 here. In Sakov et al. (2012), it was
23 proposed that a system should in fact not exceed 10 % of the ensemble size to
24 avoid a collapse of the ensemble.

25 In Fig. 7, we are presenting the mean of the spatial DFS (Eq.8) in March and
26 November.

$$27 \quad \overline{DFS}_j = \sqrt{\frac{1}{M} \sum_{i=1}^M DFS_{ij}^2} \quad (8).$$

28 where M is the total number of assimilating times within the specific time
29 period (here 4). In the Arctic the total DFS is dominated by the ice
30 concentration with large value near the ice edge. The DFS for SMOS-Ice is
31 comparatively smaller. It is larger in March than in November. However, in
32 some region, the monthly DFS of SMOS-ice reaches value larger than 2.



1 Figures of 8 and 9 show the relative contribution of each observational data set
2 calculated as follows:

$$3 \quad \mathbf{RDFS}_j = 100\% \times \overline{\mathbf{DFS}_j} / \sum_{k=1}^O \overline{\mathbf{DFS}_k} \quad (9).$$

4 where O is the number of the used observation types. As expected, the
5 assimilation of ice concentration dominates the total DFS, while the impacts of
6 SST and SLA are limited to the region that are not ice covered. Profiles in the
7 Arctic are the ice-tethered profiles. They have a very large impact but that are
8 very sparse. In March the SMOS-ice data has a significant impacts ($> 20\%$ of
9 the total DFS) in the Northern Barents Sea, the western Kara Sea, in the Baffin
10 Bay, in the Greenland Sea and in the Hudson Bay. In November, the relative
11 contribution is still large in the Barents Sea, the Kara Seas and the Greenland
12 Sea, but it is now also large in the Beaufort Sea, and in the Canadian
13 Archipelagos.

14

15 **6. Summary and Discussion**

16 The thickness observations of thin sea ice in the Arctic can be derived from
17 SMOS brightness temperature at 1.4 GHz (Tian-Kunze, et al., 2014;
18 Kaleschke et al., 2016). This data set is available in near real time since 2010
19 at daily frequency. This study investigates the impact of assimilating this data
20 set within TOPAZ system, which is the Arctic component of the Copernicus
21 Marine Services. It is shown that for thin ice (less than 0.4 m), TOPAZ
22 reanalysis and the SMOS-Ice have comparable distribution, but TOPAZ
23 reanalysis tends to overestimate thin ice thickness, especially from January to
24 April.

25 We compare the benefit of assimilating SMOS-ice (thinner than 0.4) in
26 TOPAZ system that already assimilates ice concentration, SST, SSH and
27 temperature and salinity profiles. The comparison is carried out for two periods:
28 February-March and October-November of 2014. The study shows that the
29 assimilation of SMOS-Ice data reduces the thickness RMSD of thin sea-ice in
30 March and in November by about 11% and 22% respectively, mainly caused
31 by the reduction of the bias (too thick sea ice that seems larger in 2014 than in
32 previous years). As in Yang et al. (2015) we find that there is slight



1 improvement in the ice concentration, the RMSD for SST and SLA remains
2 unchanged but not degraded.

3 In this study, the DFS has been used to evaluate the relative contributions of
4 assimilated observations to the reduction of error in TOPAZ system. The
5 SMOS-Ice data have a smaller impact than ice concentration, but has relative
6 high contributions in some areas. In the Greenland Sea, the Kara Sea and the
7 Barents Sea, a significant contribution (defined as larger than 20 % of the total
8 impact from all observations) is found both in March and November. In the
9 Baffin Bay and Hudson Bay, the significant contributions are also found in
10 March. In the Beaufort Sea and in the Canadian archipelagos, there is a large
11 contribution in November.

12 To conclude, we found that the assimilation of SMOS-ice has an important role
13 to reduce the thick biases at some regions for the sea ice thickness in the
14 Arctic. It is also encouraging that the assimilation of this data set does not
15 degrade other variables (SST, SLA, ICEC and ice drift). This suggests that
16 SMOS-Ice can be assimilated without degradation of other skills in the
17 operational forecasting system and included in the future runs or the extension
18 of the reanalysis. However, further work needs to be done to better
19 understand the uncertainty of the assimilated sea ice thickness from the
20 SMOS-Ice. Some information, like a measure of “saturation ratio” which is
21 defined by the relationship of the variable L-band penetration depth and the
22 maximal retrieval thickness as a function of temperature and salinity, may be
23 helpful for the next assimilation running.

24 In additional, the satellite sensor of CryoSat-2 provides data of the freeboard
25 height can be complementary with the sensor of SMOS (Kaleschke et al.,
26 2010). The new sea ice thicknesses derived from the combined information
27 from SMOS and CryoSat-2 will be soon available (Kaleschke et al., 2015).
28 Hebert et al. (2016) presented a blended sea ice thickness from Cryosat-2 and
29 SMOS, in which the thicknesses thinner than 0.45 m are kept from SMOS. The
30 blended sea ice thickness has been implemented into the U.S Navy Arctic Cap
31 Nowcast/Forecast System (ACNFS) for one year. This kind combined
32 observations for sea ice thickness may provide more reliable estimates, and
33 give more potential abilities to improve the forecast performance in an
34 operational ocean system by data assimilation.



1

2 **Acknowledgment**

3 This study was supported by the projects (ESA contracts
4 4000101476/10/NL/CT and 4000112022/14/I-AM) and the CPU time from the
5 Norwegian Supercomputing Project (NOTUR II grant number nn2993k).

6

7

8 **Reference:**

9

- 10 Bentsen, M., Evensen, G., Drange, H., and Jenkins, A. D.: Coordinate transformation on a
11 sphere using conformal mapping, *Mon. Weather Rev.*, 127, 2733–2740,
12 doi:[http://dx.doi.org/10.1175/1520-0493\(1999\)127<2733:CTOASU>2.0.CO;2](http://dx.doi.org/10.1175/1520-0493(1999)127<2733:CTOASU>2.0.CO;2), 1999.
- 13 Bleck, R.: An oceanic general circulation model framed in hybrid isopycnic-Cartesian coordi-
14 nates, *Ocean Model.*, 4, 55–88, doi:10.1016/S1463-5003(01)00012-9, 2002.
- 15 Bouillon, S., Fichefet, T., Legat, V., and Madec, G.: The elastic-viscous-plastic method revised.
16 *Ocean Modell.* 7, 2-12. doi:10.1016/j.ocemod.2013.05.013, 2013.
- 17 Cardinali, C., Pezzulli, S., and Andersson, E.: Influence-matrix di-agnostic of a data
18 assimilation system, *Q. J. R. Meteorol. Soc.*, 130, 2767–2786, doi:10.1256/qj.03.205,
19 2004.
- 20 Chapman, W.L., and Walsh, J. E.: Recent variations of sea ice and air temperature in high
21 latitudes, *Bull. A mer. Meteorol. Soc.*, 74, 33 —47, doi: [http://dx.doi.org/10.1175/1520-0477\(1993\)074<0033:RVOSIA>2.0.CO;2](http://dx.doi.org/10.1175/1520-0477(1993)074<0033:RVOSIA>2.0.CO;2), 1993.
- 22
23 Chassignet, E. P., Hurlburt, H. E., Metzger, E. J., Smedstad, O. M., Cummings, J., Halliwell, G.
24 R., Bleck, R., Baraille, R., Wallcraft, A. J., Lozano, C., Tolman, H. L., Srinivasan, A.,
25 Hankin, S., Cornillon, P., Weisberg, R., Barth, A., He, R., Werner, F., and Wilkin, J.: US
26 GODAE: Global Ocean Prediction with the HYbrid Coordinate Ocean Model (HYCOM),
27 *Oceanography*, 22, 64–75. Doi:10.5670/oceanog.2009.39, 2009.
- 28 Chassignet, E. P., Smith, L. T., and Halliwell, G. R.: North Atlantic Simulations with the
29 Hybrid Coordinate Ocean Model (HYCOM): Impact of the vertical coordinate choice,
30 reference pressure, and termobaricity, *J. Phys. Oceanogr.*, 33, 2504–2526.
31 Doi: [http://dx.doi.org/10.1175/1520-0485\(2003\)033<2504:NASWTH>2.0.CO;2](http://dx.doi.org/10.1175/1520-0485(2003)033<2504:NASWTH>2.0.CO;2), 2003.
- 32 Connor, L. N., Laxon, S. W., Ridout, A. L., Krabill, W. B., and McAdoo, D. C.: Comparison of
33 Envisat radar and airborne laser altimeter measurement over Arctic sea ice. *Remote
34 Sensing of Environment.* 113, 563-570, doi:10.1016/j.rse.2008.10.015, 2009
- 35 Dee, D.P., Uppala, S. M., Simmons, A. J., Berrisford, P., et al.: The ERA-Interim reanalysis:
36 configuration and performance of the data assimilation system, *Quart. J. Roy. Meteor.
37 Soc.*, 137, 553–597. Doi: 10.1002/qj.828, 2011
- 38 Donlon, C.J., Martin, M., Stark, J. D., Roberts-Jones, J., and Fiedler, E.: The Operational Sea
39 Surface Temperature and Sea Ice Analysis (OSTIA) system. *Rem. Sens. of Environment*,
40 116: 140-158. doi:10.1016/j.rse.2010.10.017, 2012.
- 41 Drange, H., and Simonsen, K.: Formulation of air-sea fluxes in the ESOP2 version of MICOM,
42 Technical Report No. 125 of Nansen Environmental and Remote Sensing Center, 1996.
- 43 Forsberg, R. and Skourup, H.: Arctic Ocean gravity, geoid and sea-ice freeboard heights from
44 ICESat and GRACE. *Geophys. Res. Lett.*, 32(21), L21502. doi:10.1029/2005GL023711,
45 2005.
- 46 Giles, K. A., Laxon, S. W., Wingham, D. J., et al.: Combined airborne laser and radar altimeter
47 measurements over the Fram Strait in May 2002. *Remote Sensing of Environment.* 111(2-
48 3), 182-194, doi:10.1016/j.rse.2007.02.037, 2007.
- 49 Giles, K. A., Laxon, S. W., and Ridout, A. L.: Circumpolar thinning of Arctic sea ice following
50 the 2007 record ice extent minimum, *Geophys. Res. Lett.*, 35, L22502, doi:10.1029/
51 2008GL035710, 2008.
- 52 Guemas, V., Wrigglesworth, E. B., Chevallier, M., et al.: A review on Arctic



- 1 sea- icepredictability and prediction on seasonal to decadal timescales. Q. J. R.
 2 Meteorolog. Soc., 142(695), dio:10.1002/qj.2401, 2014.
- 3 Hebert, D., Posey, P., Allard, R. Wallcraft, A., Metzger, E. J., and Li, L.: High resolution sea
 4 ice data assimilation and verification in the U.S. Navy Arctic Cap Nowcast/Forecast
 5 System 30 (ACNFS) and Global Ocean Forecast System (GOFS) 3.1, 7th IICWG Data
 6 assimilation and PPP ice verification Workshop, Frascati, Italy. 2016.
- 7 Heygster, G., Hendricks, S., Kaleschke, L., Maass, N., Mills, P., Stammer, D., Tonboe, R.
 8 T.,and Haas, C.:*L-Band Radiometry for Sea-Ice Applications*, Final Report for ESA
 9 ESTEC Contract 21130/08/NL/EL, Institute of Environmental Physics, University of
 10 Bremen, November 2009, 219 pp, 2009.
- 11 Hunke, E. C., and Dukowicz, J. K.: An elastic-viscous-plastic model for sea ice dynamics, J.
 12 Phys. Oceanogr., 27, 1849–1867. Doi: [http://dx.doi.org/10.1175/1520-](http://dx.doi.org/10.1175/1520-0485(1997)027<1849:AEVPMF>2.0.CO;2)
 13 [0485\(1997\)027<1849:AEVPMF>2.0.CO;2](http://dx.doi.org/10.1175/1520-0485(1997)027<1849:AEVPMF>2.0.CO;2), 1997.
- 14 Huntemann, M., Heygster, G., Kaleschke, L., Krumpfen, T., Mä'kynen M., and Mrusch, M.:
 15 Empirical sea ice thickness retrieval during the freeze-up period from SMOS high incident
 16 angle observations, The Cryosphere, 8, 439-451, doi:10.5194/tc-8-439-2014, 2014
- 17 Kaleschke, L., Maaß, N., Haas, C., Hendricks, S., Heygster, G., and Tonboe, R.: A sea-ice
 18 thickness retrieval model for 1.4 GHz radiometry and application to airborne
 19 measurements over low salinity sea-ice, The Cryosphere, 4, 583 – 592. Doi: 10.5194/tc-4-
 20 583-2010, 2010.
- 21 Kaleschke, L., Tian-Kunze, X., Maaß, N., Mä'kynen M., and Drusch, M.: Sea ice thickness
 22 retrieval from SMOS brightness temperatures during the Arctic freeze-up period. J.
 23 Geophys. Lett. 39, L05501, doi: 10.1029/2012GL050916, 2012
- 24 Kaleschke, L., Tian-Kunze, X., Maaß, N., Ricker, R., Hendricks, S., and Drusch, M.: Improved
 25 retrieval of sea ice thickness from SMOS and Cryosat-2. Proceedings of 2015
 26 International Geoscience and Remote Sensing Symposium IGARSS. [Doi:
 27 10.1109/IGARSS.2015.7327014](http://dx.doi.org/10.1109/IGARSS.2015.7327014), 2015.
- 28 Kaleschke, L., Tian-Kunze, X., Maaß, N., et al.: SMOS sea ice product: Operational
 29 application and validation in the Barents Sea marginal ice zone. Remote Sensing of
 30 Environment, doi:10.1016/j.rse.2016.03.009, 2016.
- 31 Karl, T. R., Arguez, A., Huang, B., Lawrimore, J. H., McMahon, J. R., Menne, M. J., Peterson,
 32 T. C., Vose, R. S., and Zhang, H.-M.: Possible artifacts of data biases in the recent global
 33 surface warming hiatus. Science, 348 (6242), 1469-1472.doi: 10.1126/science.aaa5632,
 34 2015.
- 35 Korosov, A., Counillon, F., and Johannessen, J. A.: Monitoring the spreading of the Amazon
 36 freshwater plume by MODIS, SMOS, Aquarius, and TOPAZ. J .Geophys. Res., 120, 268-
 37 283, doi:10.1002/2014JC010155, 2015.
- 38 Kurtz, N. T., Markus, T., Cavalieri, D. J., Sparling, L. C., Krabill, W. B., Gasiewski, A. J., and
 39 Sonntag, J. G.: Estimation of sea ice thickness distributions through the combination of
 40 snow depth and satellite laser altimetry data, J. Geophys. Res., 114, C10007,
 41 doi:10.1029/2009JC005292, 2009.
- 42 Kurtz, N. T., Farrell, S. L., Studinger, M., Galin, N., Harbeck, J. P., Lindsay, R., Onana, V. D.,
 43 Panzer, B., and Sonntag, J. G.: Sea ice thickness, freeboard, and snow depth products
 44 from Operation IceBridge airborne data. The Cryosphere 7: 1035-1056. doi:10.5194/tc-7-
 45 1035-2013, 2013.
- 46 Kwok, R., and Rothrock, D.: Decline in Arctic sea ice thickness from submarine and ICESat
 47 records: 1958–2008, Geophys. Res. Lett., 36, L15501, doi:10.1029/2009GL039035, 2009.
- 48 Johnson, M., Proshutinsky A., Aksenov Y., Nguyen A. T., Lindsay R., Haas C., Zhang J.,
 49 Diansky N., Kwok R., et al.: Evaluation of Arctic sea ice thickness simulated by Arctic
 50 Ocean Model Intercomparison Project models. J.Geophys. Res., 117(C8),
 51 doi:10.1029/2011JC007257, 2012.
- 52 Johannessen, J. A., Raj, R.P., Nilesen, J. E. Ø., Pripp, T., Knudsen, P., Counillon, F., Stammer,
 53 D., Bertino, L., Andersen, O. B., Serra, N., and Koldunov, N.: Toward Improved
 54 Estimation of the Dynamic Topography and Ocean Circulation in the High Latitude and
 55 Arctic Ocean: The Importance of GOCE. SurvGeophys, doi:10.1007/s10712-013-9270-y,



- 1 2014.
- 2 Johannessen, O. M., Shalina, E. V., and Miles, M. W.: Satellite evidence for an Arctic Sea ice
3 cover in transformation, *Science*, 286, 1937–1939. Doi:10.1126/science.286.5446.1937,
4 1999.
- 5 Laxon, S., Peacock, N., and Smith, D.: High interannual variability of sea ice thickness in the
6 Arctic region, *Nature*, 425, 947–950, doi:10.1038/nature02050, 2003.
- 7 Laxon, S. W., Giles, K. A., Ridout, A. L., Wingham, D. J., Willatt, R., Cullen, R., Kwok, R.,
8 Schweiger, A., Zhang, J., Haas, C., Hendricks, S., Krishfield, R., Kurtz, N., Farrell, S.,
9 and Davidson, M.: CryoSat-2 estimates of Arctic sea ice thickness and volume, *Geophys.*
10 *Res. Lett.*, 40, 732–737, doi:10.1002/grl.50193, 2013.
- 11 Lien, V. S., Hjøllø, S. S., Skogen, M. D., Svendsen, E., Wehde, H., Bertino, L., Counillon, F.,
12 Chevallier, M., and Garric, G.: An assessment of the added value from data assimilation
13 on modelled Nordic Seas hydrography and ocean transports, *Ocean Modelling*,
14 doi:10.1016/j.ocemod.2015.12.010, 2016.
- 15 Locarnini, R., Antonov, J., and Garcia, H.: World Ocean Atlas 2005, Volume 1: Temperature.,
16 vol. 61, US Dept. of Commerce, National Oceanic and Atmospheric Administration, 2006.
- 17 Mecklenburg, S., Drusch, M., Kaleschke, L., Rodriguez-Fernandez, N., Reul, N., Kerr, Y.,
18 Font, J., Martin-Neira, M., Oliva, R., Daganzo-Eusebio, E., Grant, J. P., Sabia, R.,
19 Macelloni, G., Rautiainen, K., Fauste, J., de Rosnay, P., Munoz-Sabater, J., Verhoest, N.,
20 Lievens, H., Delwart, S., Crapolicchio, R., de la Fuente, A., and Kornberg, M.: ESA's Soil
21 Moisture and Ocean Salinity mission: From science to operational applications, *Remote*
22 *Sensing of Environment*, <http://dx.doi.org/10.1016/j.rse.2015.12.025>, 2016.
- 23 Melsom, A., Counillon, F., LaCasce, J. H., and Bertino, L.: Forecasting search areas using
24 ensemble ocean circulation modeling. *Ocean Dynamics*, 62(8), 1245–1257, 2012.
- 25 Outten, S. and Esau, I.: A link between Arctic sea ice and recent cooling trends over Eurasia,
26 *Climatic Change*, 110, 1069–1075, doi:10.1007/s10584-011-0334-z, 2012.
- 27 Ricker, R., Hendricks, S., Helm, V., et al.: Sensitivity of CryoSat-2 Arctic sea-ice freeboard
28 and thickness on radar-waveform interpretation, *The Cryosphere*, 8, 1607–1622,
29 doi:10.5194/tc-8-1607-2014, 2014.
- 30 Rodgers, C.: Inverse methods for atmospheres: theory and practice, World Scientific, 2000.
- 31 Roemmich, D., Church, J., Gilson, J., Monselesan, D., Sutton, P., and Wijffels, S.: Unabated
32 planetary warming and its ocean structure since 2006. *Nature Climate Change* 5, 240–245.
33 doi:10.1038/nclimate2513, 2015.
- 34 Rothrock, D.A., Yu, Y., and Maykut, G. A.: Thinning of the Arctic sea ice cover, *Geophys.*
35 *Res. Lett.*, 26, 3469 —3472. Doi:10.1029/1999GL010863, 1999.
- 36 Sakov, P., and Oke, P. R.: A deterministic formulation of the ensemble Kalman filter: an
37 alternative to ensemble square root filters. *Tellus A*, 60(2):361–371, doi:10.1111/j.1600-
38 0870.2007.00299.x, 2008.
- 39 Sakov, P., Evensen, G., and Bertino, L.: Asynchronous data assimilation with the EnKF. *Tellus*
40 *A*, 62(1), 24–29. Doi:10.1111/j.1600-0870.2009.00417.x, 2010.
- 41 Sakov, P., Counillon, F., Bertino, L., Lisæter, K. A., Oke, P. R., and Korabely, A.: TOPAZ4:
42 an ocean-sea ice data assimilation system for the North Atlantic and Arctic. *Ocean*
43 *Science*, 8:633–656, doi:10.5194/os-8-633-2012, 2012.
- 44 Schweiger, A., Lindsay, R., Zhang, J., Steels, M., Stern, H., and Kwok, R.: Uncertainty in
45 modeled Arctic sea ice volume, *J. Geophys. Res.*, 116, C00D06, doi:10.1029/2011JC007084,
46 2012.
- 47 Screen, J. A., and Simmonds, I.: Declining summer snowfall in the Arctic: Causes, impacts and
48 feedbacks, *Clim. Dynam.*, 38, 2243–2256, doi:10.1007/s00382-011-1105-2, 2012.
- 49 Serreze, M., Walsh, J., Chapin, F., Osterkamp, T., Dyrurgerov, M., Romanovsky, V., Oechel,
50 W., Morrison, J., Zhang, T., and Barry, R. G.: Observational evidence of recent changes
51 in the northern high latitude environment, *Climate Change*, 46, 159 —207. Doi:
52 10.1023/A:1005504031923, 2000.
- 53 Shimada, K., Kamoshida, T., Itoh, M., Nishino, S., Carmack, E., McLaughlin, F., Zim-
54 mermann, S., and Proshutinsky, A.: Pacific Ocean inflow: Influence on catastrophic
55 reduction of sea ice cover in the Arctic Ocean, *Geophys. Res. Lett.*, 33(8),



- 1 doi:10.1029/2005GL025624, 2006.
- 2 Simmons, A., Uppala, S., Dee, D., and Kobayashi, S.: ERA-Interim: New ECMWF reanalysis
- 3 products from 1989 onwards, ECMWF Newsletter, 110-Winter 2006/07, 25-35, 2007.
- 4 Smith, G. C., Roy, F., Reszka, M., Colan, D. S., He, Z., Deacu, D., et al.: Sea ice forecast
- 5 verification in the Canadian Global Ice Ocean Prediction System. *Quart. J. Roy. Meteor.*
- 6 *Soc.*, doi:10.1003/qj.2555, 2015.
- 7 Steele, M., Morley, R., and Ermold, W.: PHC: A global ocean hydrography with a high-quality
- 8 Arctic Ocean, *J. Climate*, 14, 2079–2087. Doi:[http://dx.doi.org/10.1175/1520-](http://dx.doi.org/10.1175/1520-0442(2001)014<2079:PAGOHW>2.0.CO;2)
- 9 0442(2001)014<2079:PAGOHW>2.0.CO;2, 2001.
- 10 Tian-Kunze, X., Kaleschke, L., Maaß, N., Mäkynen, M., Serra, N., Drusch, M., and Krumpen,
- 11 T.: SMOS-derived sea ice thickness: algorithm baseline, product specifications and initial
- 12 verification, *The Cryosphere*, 8, 997-1018, doi:10.5194/tc-8-997-2014, 2014.
- 13 Tilling, R. L., Ridout, A., and Shepherd, A.: Near real time Arctic sea ice thickness and
- 14 volume from CryoSat-2, *The Cryosphere Discuss.*, doi:10.5194/tc-2016-21, 2016.
- 15 Vandenbulcke, L., and Barth, A.: A stochastic operational forecasting system of the Black Sea:
- 16 Technique and validation. *Ocean Modell.*, 93, 7-12, doi:10.1016/j.ocemod.2015.07.010,
- 17 2015.
- 18 Winther, N.G., and Evensen, G.: A hybrid coordinate ocean model for shelf sea simulation.
- 19 *Ocean Modell.*, 13, 221–237. Doi: 10.1016/j.ocemod.2006.01.004, 2006.
- 20 Woodgate, R. A., Weingartner, T. J., and Lindsay, R.: Observed increases in Bering Strait
- 21 oceanic fluxes from the Pacific to the Arctic from 2001 to 2011 and their impacts on the
- 22 Arctic Ocean water column, *Geophys. Res. Lett.*, 39, L24603,
- 23 doi:10.1029/2012GL054092, 2012.
- 24 Xie, J., Bertino, L., Counillon, F., Lisæter, K. A., and Sakov, P.: Quality assessment of the
- 25 TOPAZ4 reanalysis in the Arctic over the period 1991-2013, 2016 (Submitted)
- 26 Yang, Q., Losa, S. N., Losch, M., Tian-Kunze, X., Nerger, L., Liu, J., Kaleschke, L., and
- 27 Zhang, Z.: Assimilating SMOS sea ice thickness into a coupled ice-ocean model using a
- 28 local SEIK filter, *J. Geophys. Res. Oceans*, 119, doi:10.1002/2014JC009963, 2014.
- 29 Zygmuntowska, M., Rampal, P., Ivanova, N., and Smedsrud, L. H.: Uncertainties in Arctic sea
- 30 ice thickness and volume: new estimates and implications for trends. *The Cryosphere*, 8,
- 31 705–720, doi:10.5194/tc-8-705-2014, 2014.



Table 1. Overview of assimilated observations in each assimilation cycle of the present TOPAZ system. All observations are retrieved from <http://marine.copernicus.eu>.

Type	Spacing	Resolution	Provider
SLA	Track	-	CLS
SST	Gridded	5 km	OSTIA from UK Met Office
In-situ T	Point	-	Ifremer + other
In-situ S	Point	-	Ifremer + other
ICEC	Gridded	10 km	OSISAF
Ice drift	Gridded	62.5 km	OSISAF

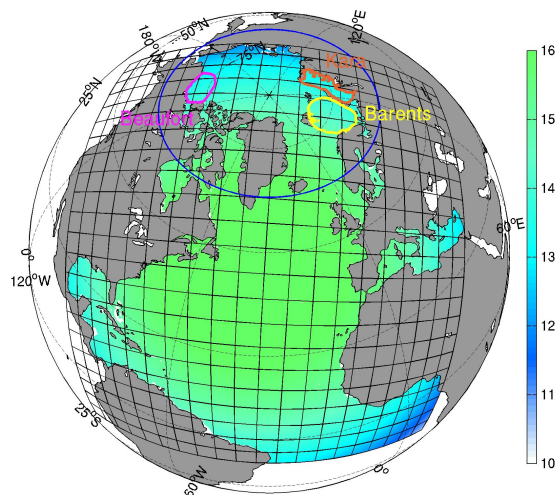


Fig. 1 TOPAZ model domain and horizontal grid resolution (km) with color shading. The blue line delimits the focused Arctic region (north of 63°N) and other color lines delimit the three marginal seas discussed in this study.

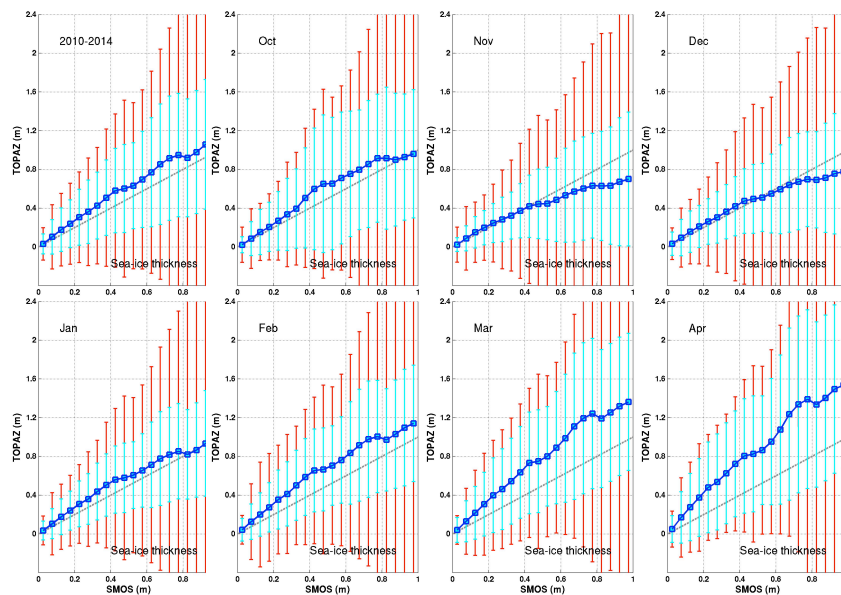


Fig. 2 Conditional expectations of TOPAZ versus SMOS-Ice (with bin of 5 cm) for the period 2010-2014 and for each month. The cyan error-bars correspond to the RMSD against all observations within each bin. The red error-bars correspond to averaged standard deviations of observation error. The gray dashed line denotes the line $y=x$.

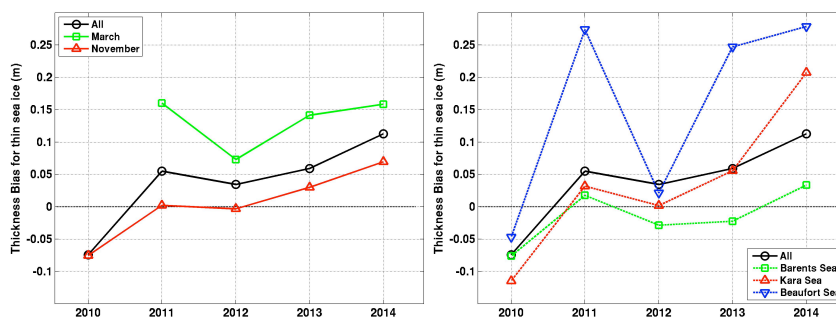


Fig. 3 Yearly thickness biases of thin sea ice from TOPAZ compared to SMOS-Ice observations. The black line represents the yearly mean bias. **Left:** the green (resp. red) line represents the mean bias for March (resp. November) of each year. **Right:** the colored lines represent the mean biases in the Barents Sea, the Kara Sea, and the Beaufort Sea.

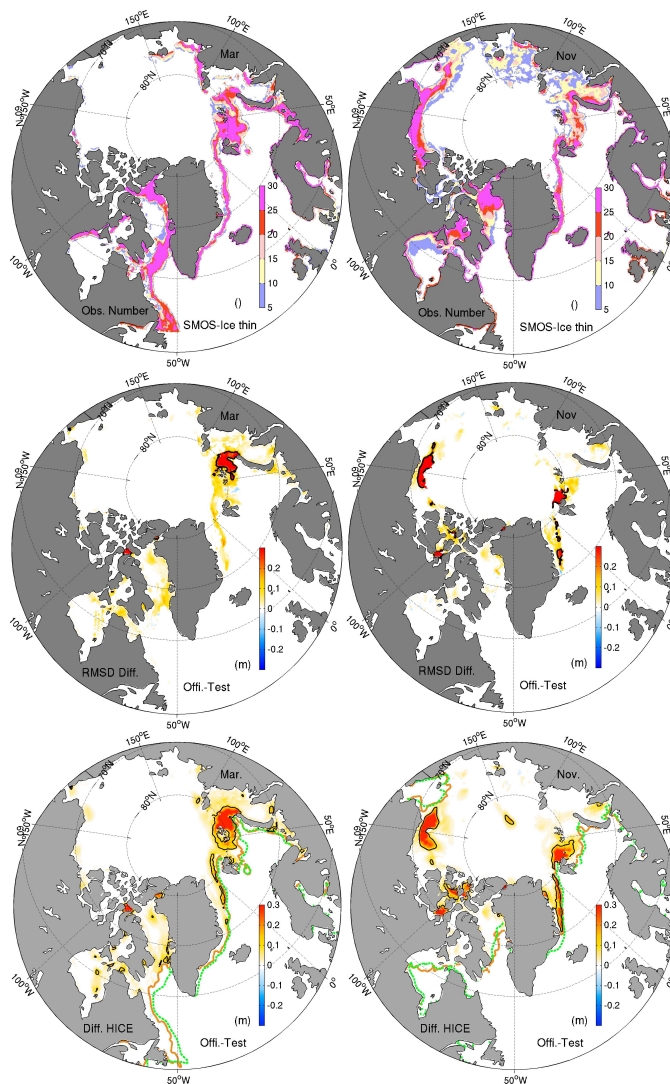


Fig. 4 Top: SMOS-Ice data assimilated in the model in March (left) and in November (right). **Middle:** Difference of RMSDs for the thin sea-ice thicknesses between the **Official Run** and the **Test Run** in March (left) and in November (right). **Bottom:** Difference of mean ice thicknesses between the two runs. The black line denotes the 0.2 m isoline, the green (resp. orange) line is the 15% concentration isoline from OSISAF (resp. the **Official Run**).

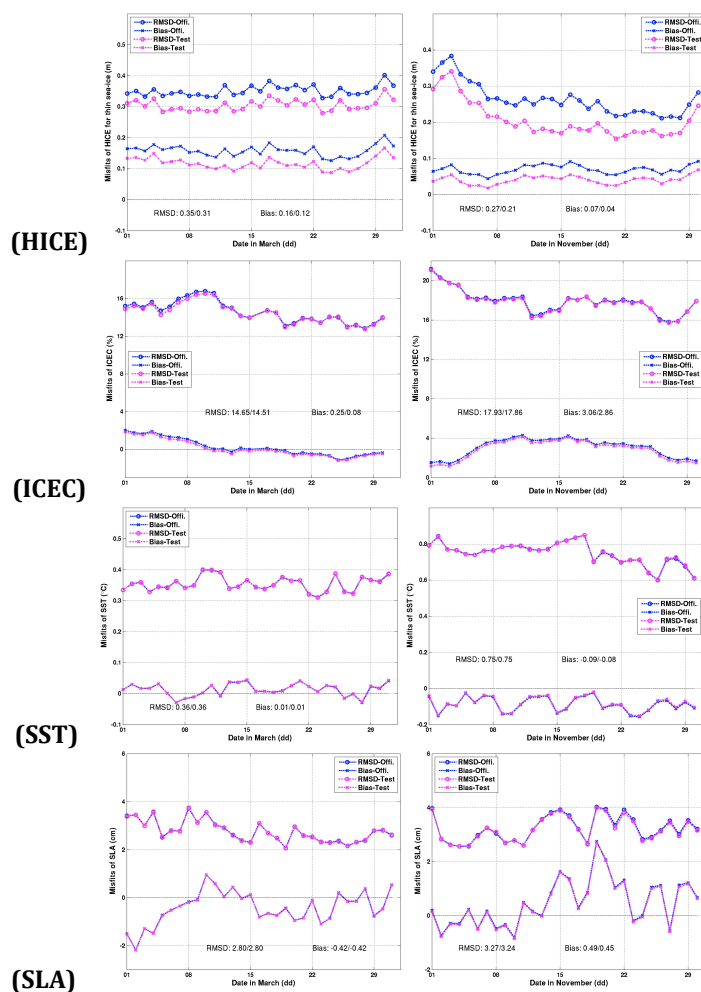


Fig. 5 Daily time series of the bias (marked with crosses) and the RMSD (marked with circles) in the whole Arctic for the **Official Run** (in blue) and the **Test Run** (in purple) for different variables in March (Left) and November (Right).

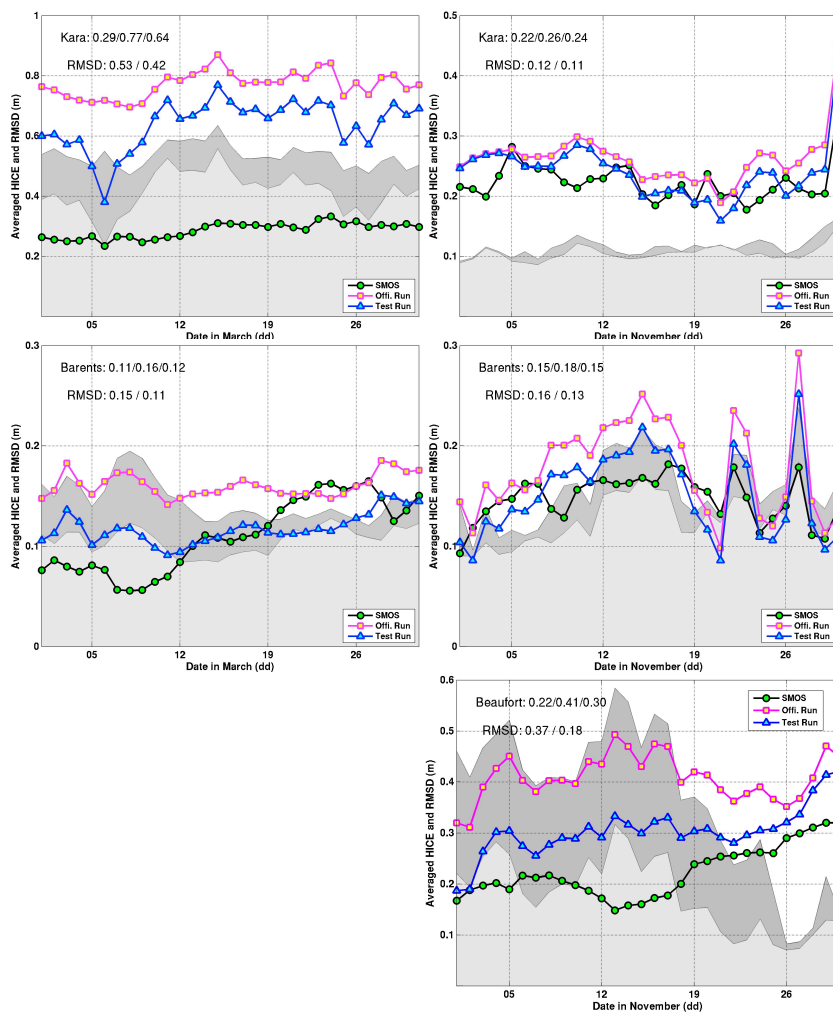


Fig. 6 Daily time series of the mean thickness of thin sea-ice in the Kara Sea (upper), the Barents Sea (middle) and Beaufort Sea (bottom) for March (*left*) and November (*right*). The light (resp. dark) gray shading is the dailyspatial RMSD of thin sea ice in the **Test Run** (resp. **Official Run**).

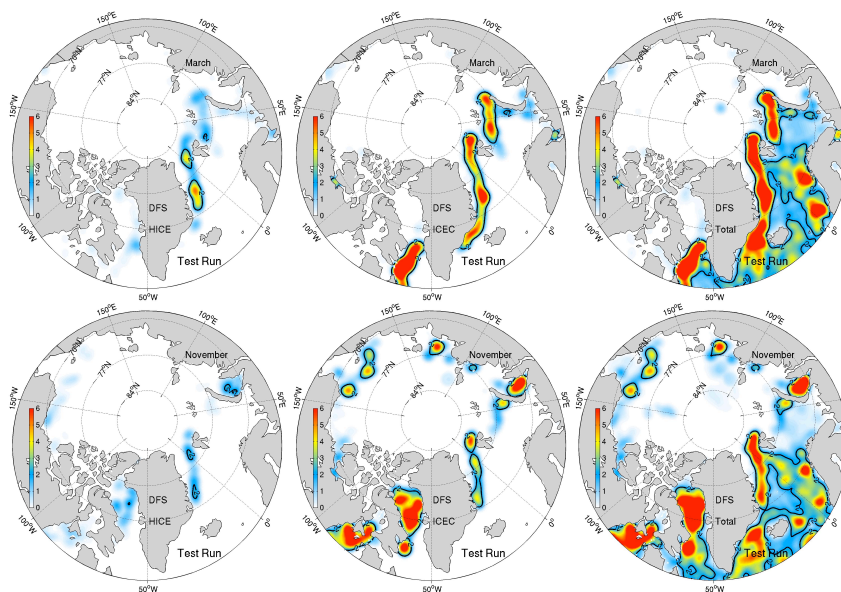


Fig. 7 Monthly averaged Degrees of Freedom for Signal (DFS) from the **Test Run** in March (*upper*) and in November (*lower*) for SMOS-Ice sea ice thickness (left), sea ice concentration (middle), and the total DFS of all ice and ocean observations (right). The black line denotes the isoline of DFS equal to 2.

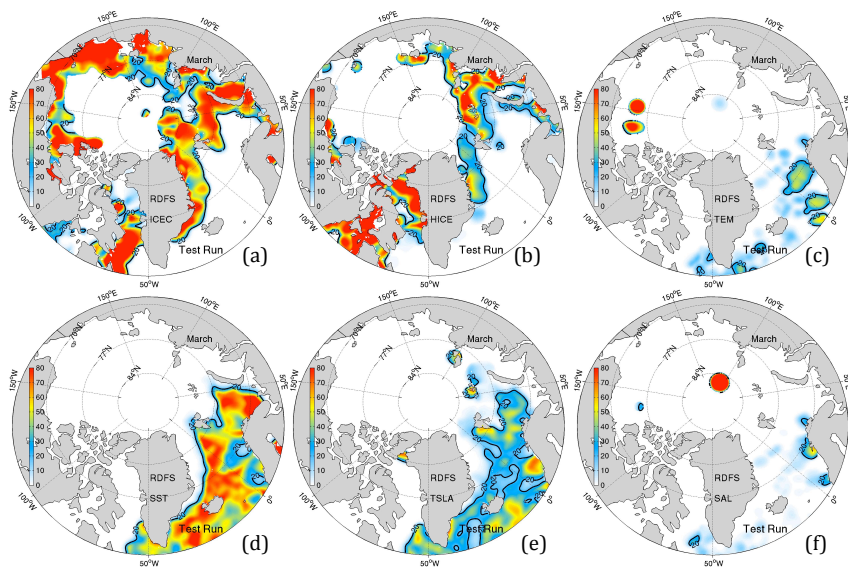


Fig. 8 Relative contributions of each observational data set in the total DFS during March 2014. Panel (a) is for sea ice concentration; (b) ice thickness from SMOS-Ice; (c) temperature profiles; (d) SST; (e) along-track SLA; (f) salinity profiles. The black line is the 20% isoline.

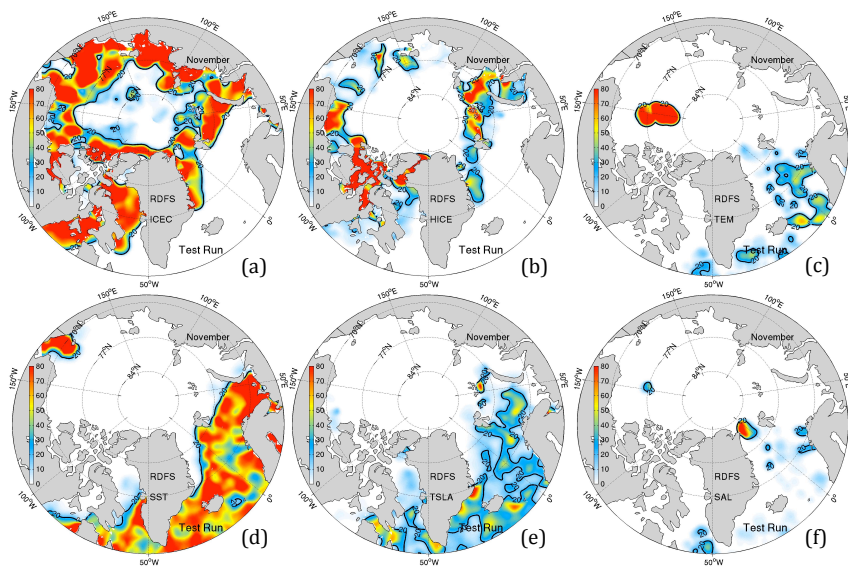


Fig. 9 Same as Figure 8 for November 2014